Available online at www.sciencedirect.com
ScienceDirect
Sensors and Actuators B 129 (2008) 391–396
SENSORS AND ACTUATORS B CHEMICAL
www.elsevier.com/locate/snb

Humidity sensing based on nanoporous polymeric photonic crystals

Jinjie Shi, Vincent K.S. Hsiao, Thomas R. Walker, Tony Jun Huang *

Department of Engineering Science and Mechanics, The Pennsylvania State University, University Park, PA 16802 USA

Received 18 June 2007; received in revised form 22 August 2007; accepted 23 August 2007
Available online 31 August 2007

Abstract

In this work, an optical humidity sensor based on a nanoporous polymeric photonic crystal (PC) is demonstrated. The PC sensing structure is created by combining a holographic interference patterning technique with a modified holographic polymer-dispersed liquid crystal system. Changes in relative humidity (RH) induce the modification of the refractive index contrast between the nanoporous and nonporous regions, and thus the transmittance and bandgap position, of the PC structure. For a PC structure with 30% porosity and a grating spacing of 220 nm, a change in the RH from 40% to 95% at 34 °C results in a redshift of 43 nm in the central wavelength at the PC bandgap and an increase from 12% to 87% in the relative transmittance at $\lambda = 600$ nm. Other performance analyses have shown that the nanoporous polymeric PC-based humidity sensor is highly stable and reproducible, exhibits minimal hysteresis, and responds relatively fast.

Keywords: Humidity sensor; Nanoporous; Photonic crystal; Holographic photopolymerization

1. Introduction

Humidity control and monitoring has attracted increasing attention in recent decades due to its importance in applications such as agriculture, environment, medicine, and the semiconductor industry [1–5]. Thus far, most studies in humidity-sensing materials have focused on porous ceramics [6–12] and polymers [13–20]. Porous polymers and ceramics have a large surface-to-volume ratio, which allows highly sensitive detection of surface alterations caused by the adsorption/desorption of water vapour. In recent years, an increasing number of studies on porous polymer-based humidity sensors have been reported, due to polymers' advantages such as low cost, ease of processing, high sensitivity, and excellent mechanical and chemical stability. Changes in the resistance, capacitance, or optical properties of porous polymers under different relative humidity (RH) can serve as humidity-sensing mechanisms [21–25].

In this work, we report the design, fabrication, and characterization of nanoporous polymeric one-dimensional photonic crystals (PC) as a platform for optical humidity sensing. Compared with the resistance- or capacitance-based humidity sensors, optical sensors are immune to electrical noises and have high detection sensitivity. The nanoporous polymeric PCs are created by combining a holographic interference patterning technique with a modified holographic polymer-dispersed liquid crystal (H-PDLC) system [26,27]. Humidity sensing is achieved through two mechanisms: changes in the RH-dependent refractive index (RI) contrast between the nanoporous and nonporous regions, and reversible swelling of the polymeric structure at high RH regions. Both mechanisms change the transmission intensity and the bandgap position of the PC structures. The nanoporous polymeric PC-based humidity sensors we demonstrate in this paper present advantages such as convenient fabrication process, amenability for miniaturization, high detection sensitivity, excellent stability and reproducibility over a wide range of RH, minor hysteresis, and fast response time.

2. Experiment

2.1. Sample fabrication

Nanoporous polymeric one-dimensional PC structures were fabricated through a holographic photopolymerization process [28–30]. The fabrication setup is shown in Fig. 1. A homogeneous pre-polymer syrup was formed by thoroughly mixing a monomer (60 wt.% dipentaerythritol hydroxypentaacrylate from Aldrich), a photo-initiator (1 wt.% Rose Bengal from Spectra Group Limited), a co-initiator (3 wt.% *N*-phenylglycine

* Corresponding author. Tel.: +1 814 863 4209; fax: +1 814 865 9974.
E-mail address: junhuang@psu.edu (T.J. Huang).

0925-4005/$ – see front matter © 2007 Elsevier B.V. All rights reserved.
doi:10.1016/j.snb.2007.08.037

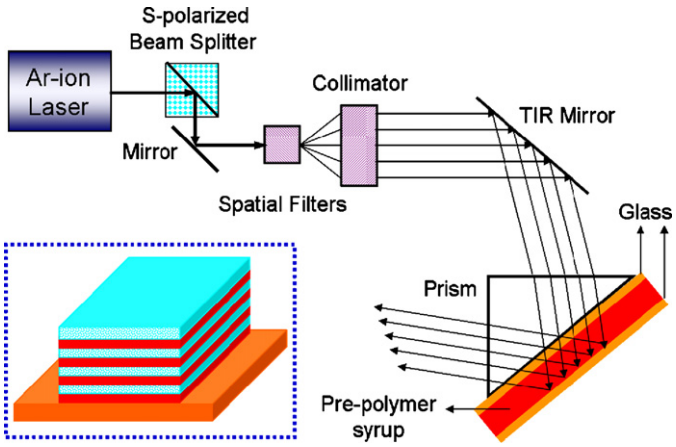

Fig. 1. Schematic of the experimental setup for the fabrication of a nanoporous polymeric one-dimensional PC. Optical components, including an argon ion laser, a beam splitter, spatial filters and collimators, were precisely positioned on an optical table. A holographic interference pattern formed on the pre-polymer syrup sandwiched between two glass slides. The inset is a schematic of a nanoporous polymeric one-dimensional PC situated on a glass substrate.

from Aldrich), liquid crystals (15 wt.% TL213 from Merck), non-reactive solvent (15 wt.% toluene from Aldrich), and 3-Aminopropyltriethoxysilane (APTES, 6 wt.% from Aldrich). The syrup was then sandwiched between two pieces of glass. The distance between the two glass slides was precisely controlled by adding microbeads (3 μm in diameter) at the edge of the syrup, thus defining the thickness of the PC structure. A 100 mW argon ion laser ($\lambda = 514$ nm, 10% P-polarized and 90% S-polarized) was used to generate an incident beam. In order to achieve a better interference pattern, the incident laser beam was split by an S-polarized beam splitter to remove the P-polarized component. After being filtered and collimated, the laser beam was guided to pass into a prism. Thus, the incident beam and its total internal reflection created an interference pattern in the syrup. A one-dimensional PC was fabricated by periodic modulation of the high and low optical intensities in the interference pattern. The modulation period of the polymeric PC was controlled by tuning the incident angle of the collimated beam. After being exposed to the interference patterning for 30 s, the samples were post-cured for 24 h in a chemical fume hood. Upon separating the sample from the cover slide, a nanoporous polymeric PC structure situated on a glass slide was obtained (schematic is shown in the insert of Fig. 1).

Fig. 2(a) and (b) shows the cross-sectional morphology of a nanoporous polymeric PC sample, observed by bright field transmission electron microscopy (BF-TEM) and scanning electron microscopy (SEM), respectively. One of the nanoporous regions is enclosed by a dashed square in both the SEM and the TEM images. The pore diameters range from a few nanometers to tens of nanometers, and the porosity of the polymeric PC structure is ~30%.

2.2. Measurement principle

The bandgap characteristic of a PC is determined by its RI contrast and filling ratio [31,32]. For the nanoporous polymeric PC structure used in this work, the RI contrast between the nanoporous and nonporous regions plays a key role in its bandgap behaviour. With increasing RH, the nanoporous regions adsorb water molecules and the RI of these regions increases. Meanwhile, the nonporous regions barely adsorb water molecules and the RI remains constant. As a result, the RI contrast between the nanoporous and nonporous regions decreases, the bandgap position redshifts, and the transmittance at the bandgap increases. In addition, at high RH regions, minor reversible swelling of the polymeric PC structure occurs, causing changes in the filling ratio, the bandgap position, and the transmittance. Thus, the humidity sensing of our nanoporous polymeric PC structures is based on two mechanisms: changes in the RH-dependent RI contrast between the nanoporous and nonporous regions, and reversible swelling of the polymeric structure at high RH regions.

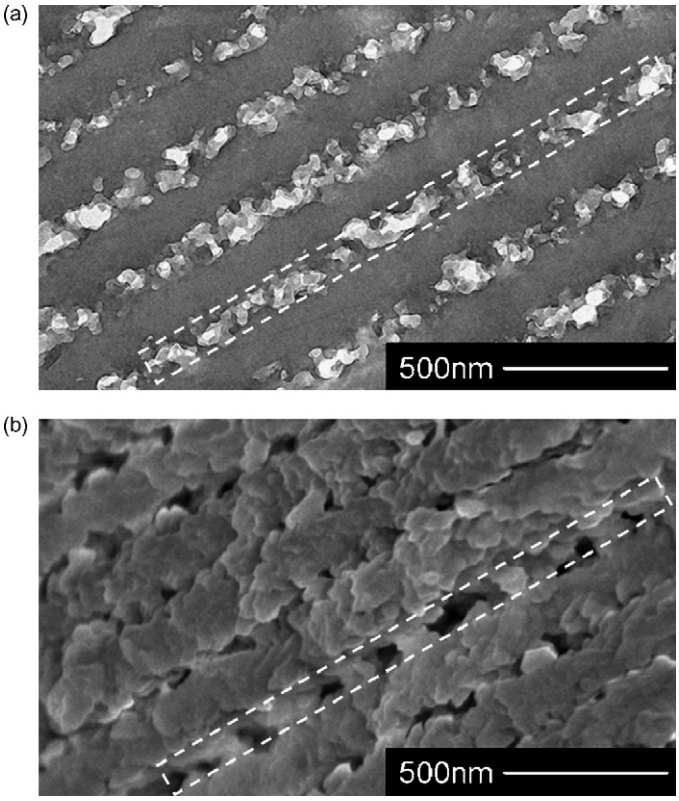

Fig. 2. (a) TEM and (b) SEM images of the cross-sectional morphology of a nanoporous polymeric one-dimensional PC. The grating spacing of the PC is about 220 nm. Dashed squares are used in both (a) and (b) to enclose one of the nanoporous regions.

2.3. Measurement setup

Fig. 3 depicts the schematic of the optical measurement setup for humidity sensing. White light produced by a halogen lamp (LS-1 Tungsten Halogen Light Source, Ocean Optics Co.) was used as the source beam in the experiments. Two optical fibres were aligned on both sides of a glass/PC sample using fibre holders. The fibres were fixed in the fibre holders using connectors (SMA 905, Ocean Optics Co.) with integrated collimating lenses (200–2000 nm 74-UV Collimating lens, Ocean Optics

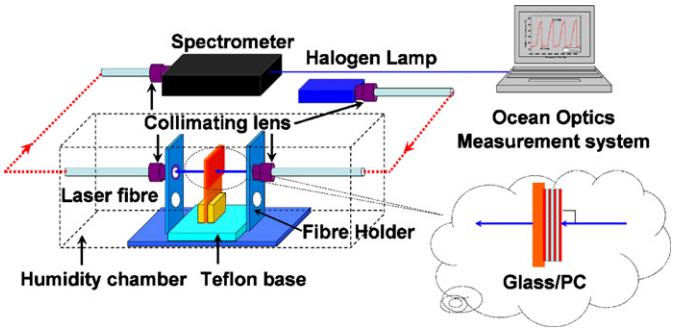

Fig. 3. Schematic of the humidity-sensing measurement setup. The polymeric PC structure coated on a glass substrate was fixed upon a Teflon base, and two optical fibres (source and readout) were aligned by fibre holders and located within a humidity chamber. A halogen lamp was used to generate white incident light. An ocean optics measurement system, including spectrometer and software, recorded and analyzed output signals.

Co.). The PC sample coated on a glass substrate was fixed on a Teflon base to ensure that the PC structure was normal to the collimated light (with divergent angle less than 2°). After passing through the sample, the light was collected, collimated, and guided to a spectrometer (HR4000, Ocean Optics Co.) where the transmitted optical signal was measured for a spectral range of 400–1000 nm. A humidity chamber (ESPEC North America Inc., SH-241) was used to control the operating temperature and humidity. The RH inside the humidity chamber could be adjusted to any number between 40% and 95%. However, since the chamber required almost 15 min to adjust humidity, a smaller quartz chamber (4 cm × 4 cm × 4 cm) and an oscillating water vapour source (between 20% and 100% RH) were used to characterize the response time.

3. Results and discussion

Fig. 4(a) shows the spectral response of the nanoporous polymeric PC to different RHs at a constant temperature (34 °C). The central wavelength (λ_{Bragg}) of the photonic bandgap for the polymeric PC structure redshifts from 615 to 658 nm as the RH increases from 40% to 95%. λ_{Bragg} can be estimated using the Bragg's Law [33]:

$$\lambda_{Bragg} = 2n_{ave}\Lambda \quad (1)$$

where n_{ave} is the average refractive index and Λ is the grating spacing. At 40% RH, n_{ave} is estimated as 1.404, assuming 30% porosity, $n_{polymer} = 1.52$, $n_{air} = 1$, and $n_{water} = 1.33$. Based on Eq. (1) and the data presented in Fig. 1, the grating spacing Λ is calculated to be 219 nm, which is in excellent agreement with the TEM/SEM measurement results (~220 nm) from Fig. 2. When the RH is changed to 95%, n_{ave} is measured to be 1.459, and the grating spacing is calculated to be 225 nm, which indicates that minor swelling of the polymeric structure occurs at a high-humidity environment. In order to test the long-term stability of this polymeric PC structure at high RH, the spectra at 95% RH were recorded continuously for 4 h (Fig. 4(b)). The central wavelength and transmittance of the bandgap remains unchanged

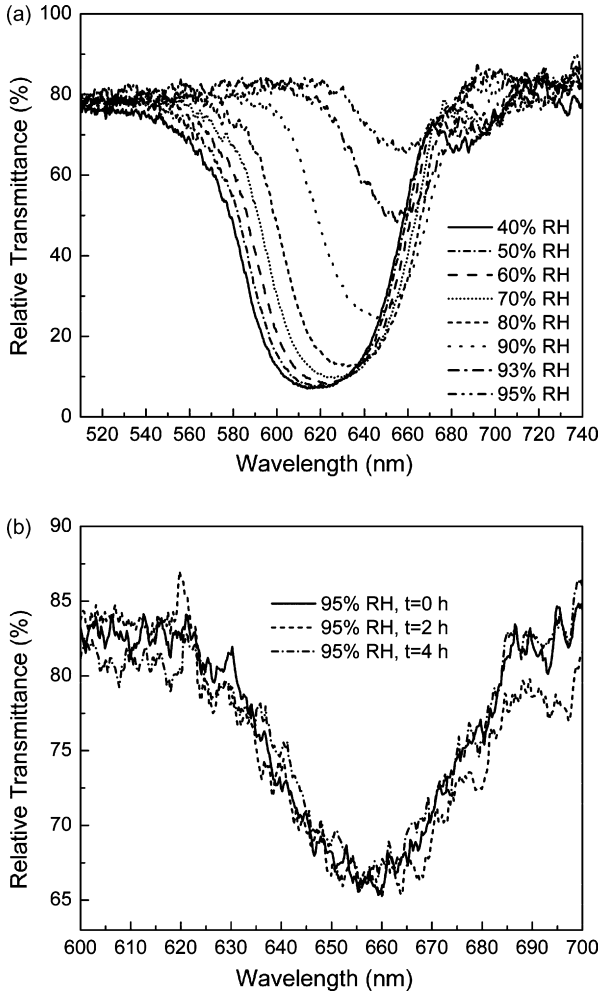

Fig. 4. (a) The transmittance spectra of a typical nanoporous polymeric PC at various RH. (b) The transmittance spectra of the PC at 95% RH recorded at $t = 0$, 2 and 4 h. The relative transmittance is the ratio of the transmitted signal to the normalized incident light.

during this time period, indicating the sensor's excellent stability at high RH regions.

Fig. 4(a) also shows that the transmittance at the PC bandgap increases with RH. This phenomenon is caused by the variations in the RI contrast between the nanoporous and nonporous regions and the minor swelling of the polymeric PC structure occurred at the high-RI regions. Higher humidity will lead to lower RI contrast, and thus, higher transmittance at the PC bandgap. As water vapour saturates the nanopores, the PC structure becomes more isotropic (the RI of water vapour is closer to that of the polymer than to that of the air voids) and its bandgap effect diminishes, resulting in increasing transmitted intensity at the bandgap. The increase of relative transmittance with RH suggests that the structure can be used as a quantitative humidity sensor. Moreover, the total transparency of the polymeric PC structure also changes as the bandgap redshifts; this mechanism makes the structure suitable as a portable colorimetric humidity sensor.

Fig. 5 depicts the dependence of transmittance on RH at several characteristic wavelengths. When the chosen characteristic

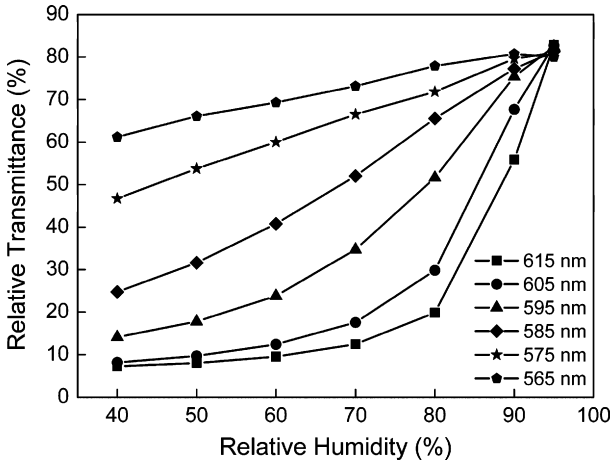

Fig. 5. The dependence of relative transmittance on RH at different characteristic wavelengths.

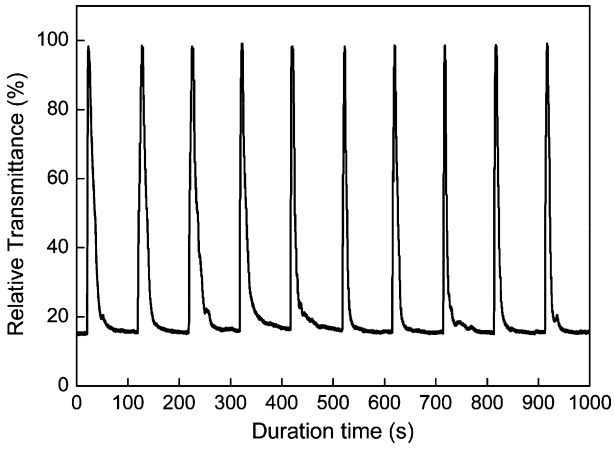

Fig. 7. The time-dependent transmittance curve ($\lambda = 595$ nm, $T = 20\,^{\circ}C$) as the RH oscillates between 20% and 100% for multiple cycles.

wavelength decreases from 615 nm (the central bandgap wavelength at 40% RH) to 565 nm, the magnitude of change in relative transmittance decreases and the relative transmittance-versus-RH curves exhibit greater linearity. These results suggest that our humidity sensors offer tunable sensitivity and linearity.

Fig. 6 shows the variation of relative transmittance ($\lambda = 600$ nm) to an RH-increasing and -decreasing cycle. When RH is changed from 40% to 95%, the relative transmittance increases from 12% to 87%, indicating the high sensitivity. Here we define the detection sensitivity as the ratio of the change in relative transmittance to the RH change ($\Delta I/\Delta$RH) at a certain wavelength in the bandgap. The sensor also demonstrates excellent stability and reversibility because its transmittance returns to the same value after one humidity increasing/decreasing cycle. Minor hysteresis is observed during the cycle. It is likely due to the different mass transport kinetics between the vapour adsorption and desorption processes. The difference in mass transport kinetics results in unequal amounts of water molecules trapped in the nanopores for the two processes (adsorption and desorption) at the same RH. The hysteresis observed in our system is considered rather minor compared to the results from previously reported studies [22,34].

The stability and repeatability of the humidity sensors over a large RH range is further demonstrated in a multi-cycle experiment in which saturated water vapour (100% RH) was periodically introduced to the smaller quartz humidity chamber where the RH was maintained to be 20%. Fig. 7 shows that as the RH periodically oscillates between 20% and 100%, the relative transmittance at the wavelength of 595 nm switches between 15% and 98%. This response is highly reproducible as we see that the difference in relative transmittance for more than 100 experimental cycles is less than 1%. Fig. 7 also shows that the humidity sensor responds more quickly to the adsorption process (from 20% to 100% RH) than to desorption (from 100% to 20% RH). This indicates that it takes longer for water molecules to diffuse from nanopores to the environment than by the opposite route. It is observed that the relative transmittance changes from 15% (almost opaque) at 20% RH to 98% (transparent) at 100% RH. This large change in transmittance enables convenient, sensitive, and cost-efficient optical measurement using a single wavelength (595 nm).

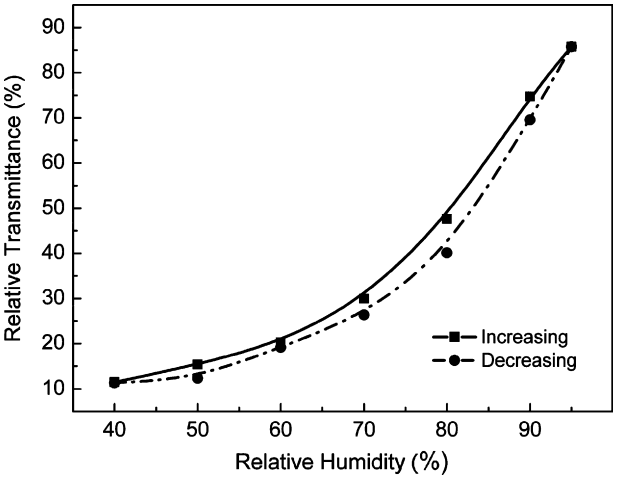

Fig. 6. Variation of the relative transmittance at 600 nm to an RH increasing/decreasing cycle. The solid squares represent the adsorption (RH increasing) process, and the circles represent the desorption (RH decreasing) process.

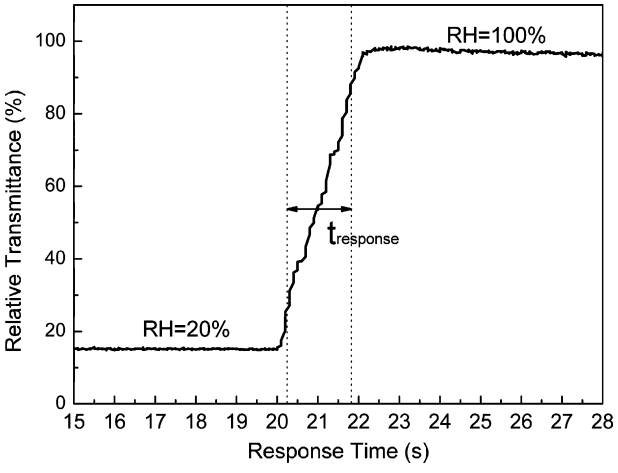

Fig. 8. The time-dependent transmittance curve ($\lambda = 595$ nm, $T = 20\,^{\circ}C$) as the RH increases from 20% to 100%.

Fig. 8 indicates that the response time for the adsorption process (from 20% to 100% RH) is about 1.5 s, while Fig. 7 shows that the desorption process takes 20–30 s. The response time and sensitivity of the sensor are dependent upon its porosity. Based on Eq. (1), the bandgap position of a PC structure is dependent upon its average RI. Higher porosity or smaller pore size leads to a larger surface-to-volume ratio and consequently, more water molecules are trapped in the nanopores. As a result, the change in the average RI is larger, and the shift of the bandgap position is more significant. By adjusting the porosity, film thickness and grating spacing, we can achieve nanoporous polymeric PC-based humidity sensors that can meet different requirements in response time and bandgap shift.

4. Conclusion

A humidity sensor based on a nanoporous polymeric PC structure is shown to be sensitive, robust, quickly responding, and cost efficient. The PC sensing structure is fabricated by combining a holographic interference patterning technique with a modified H-PDLC system. The bandgap of the PC structure shifts when water vapour penetrates the nanopores, changing the RI contrast between the porous and nonporous regions. For a PC structure with 30% porosity and a grating spacing of 220 nm, as the RH changes from 40% to 95% at 34 °C, the central wavelength of the PC bandgap redshifts 43 nm and the relative transmittance at $\lambda = 600$ nm increases from 12% to 87%. The nanoporous polymeric PC-based humidity sensor demonstrates excellent reversibility and reproducibility. When the RH oscillates between 20% and 100%, the relative transmittance at 595 nm switches between 15% and 98% reproducibly—less than 1% difference in the relative transmittance upon the same RH (20% or 100%) is observed upon hundreds of experimental cycles. The response time for the absorption process is about 1.5 s, and the desorption process takes 20–30 s. Moreover, the response time and the bandgap shift can be optimized by altering fabrication parameters, such as porosity and grating spacing.

Acknowledgements

The authors thank Pamela F. Lloyd and Timothy J. Bunning at the Air Force Research Laboratory for their help with SEM/TEM characterization, and Ashley Colletti for her help in preparing the manuscript. This research was supported in part by the start-up fund provided by The Pennsylvania State University, the Grace Woodward Grants for Collaborative Research in Engineering and Medicine, and the NSF NIRT grant (ECCS-0609128).

References

[1] Z. Chen, C. Lu, Humidity sensors: a review of materials and mechanisms, Sens. Lett. 3 (2005) 274–295.
[2] H. Arai, T. Seiyama, in: W. G¨opel (Ed.), Sensors: A Comprehensive Survey, 3, VCH, Weinheim, Germany, 1992, pp. 981–1012.
[3] R. Fenner, E. Zdankiewicz, Micro-machined water vapor sensors: a review of sensing technologies, IEEE Sens. 14 (2001) 309–317.
[4] J.R. Huang, M.Q. Li, Z.Y. Huang, J.H. Liu, A novel conductive humidity sensor based on field ionization from carbon nanotubes, Sens. Actuators A 133 (2007) 467–471.
[5] N. Yamazoe, Y. Shimizu, Humidity sensors: principles and applications, Sens. Actuators 10 (1986) 379–398.
[6] B.M. Kulwicki, Humidity sensors, J. Am. Ceram. Soc. 74 (1991) 697–708.
[7] U. Kang, K.D. Wise, A high-speed capacitive humidity sensor with on-chip thermal reset, IEEE Trans. Electron. Devices 47 (2000) 702–710.
[8] T. Seiyama, N. Yamazoe, H. Arai, Ceramic humidity sensors, Sens. Actuators 4 (1983) 85–96.
[9] E. Traversa, Ceramic sensors for humidity detection: the state-of-the-art and future developments, Sens. Actuators B 23 (1995) 135–156.
[10] A.K. Kalkan, H.D. Li, C.J. O'Brien, S.J. Fonash, A rapid-response, high-sensitivity nanophase humidity sensor for respiratory monitoring, IEEE Electron. Device Lett. 25 (2004) 526–528.
[11] E.J. Connolly, H.T.M. Pham, J. Groeneweg, P.M. Sarro, P.J. French, Relative humidity sensors using porous SiC membranes and Al electrodes, Sens. Actuators B 100 (2004) 216–220.
[12] L.M. Zambov, C. Popov, M.F. Plass, A. Bock, M. Jelinek, J. Lancok, K. Masseli, W. Kulisch, Capacitance humidity sensor with carbon nitride detecting element, Appl. Phys. A 70 (2000) 603–606.
[13] A. Tsigara, G. Mountrichas, K. Gatsouli, A. Nichelatti, S. Pispas, N. Madamopoulos, N.A. Vainos, H.L. Du, F. Roubani-Kalantzopoulou, Hybrid polymer/cobalt chloride humidity sensors based on optical diffraction, Sens. Actuators B 120 (2007) 481–486.
[14] J. Wang, K. Shi, L. Chen, X. Zhang, Study of polymer humidity sensor array on silicon wafer, J. Mater. Sci. 39 (2004) 3155–3157.
[15] T. Zajt, G. Jasiñski, B. Chachuiski, Electrical properties of polymer humidity sensor based on polyethyleneimine, Proc. SPIE 5124 (2003) 130–137.
[16] C.P.L. Rubinger, C.R. Martins, M.A. De Paoli, R.M. Rubinger, Sulfonated polystyrene polymer humidity sensor: synthesis and characterization, Sens. Actuators B 123 (2007) 42–49.
[17] T. Nomura, T. Yasuda, S. Furukawa, Humidity sensor using surface acoustic waves propagating along polymer/$LiNbO_3$ structures, Ultrason. Symp. (1993) 417–420.
[18] T. Nomura, K. Oofuchi, T. Yasuda, S. Furukawa, SAW humidity sensor using dielectric hygroscopic polymer film, Ultrason. Symp. (1994) 503–506.
[19] Y. Sakai, M. Matuguchi, Y. Sadaoka, K. Hirayama, A humidity sensor composed of interpenetrating polymer networks of hydrophilic and hydrophobic methacrylate polymers, J. Electrochem. Soc. 140 (1993) 432–436.
[20] J. Wang, F.Q. Wu, K.H. Shi, X.H. Wang, P.P. Sun, Humidity sensitivity of composite material of lanthanum ferrite/polymer quaternary acrylic resin, Sens. Actuators B 99 (2004) 586–591.
[21] M.A. Zanjanchi, Sh. Sohrabnezhad, Evaluation of methylene blue incorporated in zeolite for construction of an optical humidity sensor, Sens. Actuators B 105 (2005) 502–507.
[22] J.J. Steele, A.C. van Popta, M.M. Hawkeye, J.C. Sit, M.J. Brett, Nanostructured gradient index optical filter for high-speed humidity sensing, Sens. Actuators B 120 (2006) 213–219.
[23] B. Yang, B. Aksak, Q. Lin, M. Sitti, Compliant and low-cost humidity sensors using nano-porous polymer membranes, Sens. Actuators B 114 (2006) 254–262.
[24] B.A. Albrecht, C.H. Benson, S. Beuermann, Polymer capacitance sensors for measuring soil gas humidity in drier soils, Geotech. Test. J. 26 (2003) 3–11.
[25] Z. Yao, M. Yang, A fast response resistance-type humidity sensor based on organic silicon containing cross-linked copolymer, Sens. Actuators B 117 (2006) 93–98.
[26] S. Matsuoka, V.T. Wallder, H.L. Beauchamp, Application of holographic interference technique to mechanical studies of polymeric solids, Polym. Eng. Sci. 11 (1971) 46–50.
[27] T.J. Bunning, L.V. Natarajan, V.P. Tondiglia, R.L. Sutherland, Holographic polymer-dispersed liquid crystals (H-PDLCS), Annu. Rev. Mater. Sci. 30 (2000) 83–115.

[28] V.K.S. Hsiao, T.C. Lin, G.S. He, A.N. Cartwright, P.N. Prasad, Optical microfabrication of highly reflective volume Bragg gratings, Appl. Phys. Lett. 86 (2005) 131113.
[29] L.V. Natarajan, C.K. Shepherd, D.M. Brandelik, R.L. Sutherland, S. Chandra, V.P. Tondiglia, D. Tomlin, T.J. Bunning, Switchable holographic polymer-dispersed liquid crystal reflection gratings based on thiol-end photopolymerization, Chem. Mater. 15 (2003) 2477–2484.
[30] V.K.S. Hsiao, W.D. Kirkey, F. Chen, A.N. Cartwright, P.N. Prasad, T.J. Bunning, Organic solvent vapor detection using holographic photopolymer reflection gratings, Adv. Mater. 17 (2005) 2211–2214.
[31] E. Yablonovitch, T.J. Gmitter, Photonic band structure: the face-centered-cubic case, Phys. Rev. Lett. 63 (1989) 1950–1953.
[32] V. Berger, From photonic band gaps to refractive index engineering, Opt. Mater. 11 (1999) 131–142.
[33] H. Kogelnik, Coupled wave theory for thick hologram gratings, Bell Syst. Tech. J. 48 (1969) 2909–2947.
[34] N. Madamopoulos, S. Pispas, A. Tsigara, L. Athanasekos, G. Mountrichas, K. Gatsouli, N. Vainos, K. Kibasi, Polymer based photonic sensors for physicochemical monitoring, Proc. SPIE 5993 (2005) 599308.

Biographies

Jinjie Shi received his B.S. and M.S. degrees in microelectronics from Peking University at China in 2002 and 2005, respectively. He is currently a Ph.D. student in the Department of Engineering Science and Mechanics at The Pennsylvania State University. His research interests are in biomedical nano-electro-mechanical-systems (Bio-NEMS) and acoustic microfluidics.

Vincent K.S. Hsiao received his Ph.D. degree at the University at Buffalo, The State University of New York (SUNY). He is a postdoctoral researcher in the Department of Engineering Science and Mechanics at The Pennsylvania State University. His research is focused on holographically fabricated nanoporous polymer gratings and their applications in nanophotonics and biophotonics. After August 2007, Dr. Hsiao will be an assistant professor at the Department of Applied Materials and Optoelectronic Engineering in National Chi Nan University, Nantou, Taiwan.

Thomas R. Walker graduated in 2007 from The Pennsylvania State University with a B.S. in Engineering Science. He was recently awarded a fellowship with The National Institute of Standards and Technology (NIST) in Washington, DC. In fall of 2007, he will begin graduate studies in Engineering Science at Penn State. His current research interests include pathogen sensors to be used in food science and semiconductor metrology.

Tony Jun Huang received a Ph.D. degree in mechanical and aerospace engineering from the University of California, Los Angeles (UCLA) in 2005, and his B.S. and M.S. degrees in Energy and Power Engineering from Xi'an Jiaotong University, Xi'an, China, in 1996 and 1999, respectively. He is the James Henderson assistant professor in the Department of Engineering Science and Mechanics at The Pennsylvania State University. His research interests include biomedical nanoelectromechanicalsystems (BioNEMS), molecular mechanics, nanomaterials/nanodevices, and micro fluidics.